MagBeS-Magnetic Bearing Simulator for Analyzing and Designing Magnetically Levitated Rotors

Antje Deckert[1,a], Uwe Keller[2,b], Stefanos Fasoulas[1,c]

[1]Institute for Aerospace Engineering, TU Dresden, 01062 Dresden, Germany
[2]Centre of Competence Mechanism, Astrium GmbH, An der B31, 88090 Friedrichshafen, Germany
[a]antje.deckert@tu-dresden.de, [b]uwe.keller@astrium.eads.net, [c]stefanos.fasoulas@tu-dresden.de

Abstract: MagBeS is a Matlab based Graphical User Interface that can be used to analyze or design magnetically levitated rotors using a parametric multiphysical algorithm. The paper includes a description of the computation algorithm and shows simulation results for analyzing magnetic bearings using MagBeS, with a focus on the capability of this tool.

Keywords: Rotordynamics, Thermodynamics, Bearing Losses, Multiphysical Modeling

Introduction

Magnetic suspension of rotating machinery provides some main advantages over conventional bearing technologies and is under investigation for space mechanisms since the early 1970's [1,2]. Especially, the resulting increase of lifetime and the reduction of the induced jitter are of main interest. Furthermore, high speed applications like energy storage wheels are hardly realizable with conventional bearing concepts. Although their applicability has already been proven on selected spacecrafts, their application in space has not yet been widely established. Main reasons for that have been found in the complexity and the rare knowledge about the coupling effects of such mechatronic systems. The latter makes the prediction of the system behavior and therewith an optimized system design rather complex. Of course, tools providing advanced (e.g. finite element) analyses of the single physical domains are state of the art and also multiphysics software has been established during the last few years [3]. Nonetheless, implementing these models is time-consuming and requires a rather good knowledge of the geometry of the system. The design approaches for magnetic bearings found in literature mostly concentrate on a single physical domain, where the other influencing factors are considered as black boxes or simple linear systems.

Instead, MagBeS (Magnetic Bearing Simulator) considers three physical domains of a magnetic bearing (MB) – electromagnetism, rotordynamics, and thermodynamics. The simulator bases on a parametric approach and has been implemented in Matlab and the freeware FEMM (Finite Element Method Magnetics), which makes it applicable for a large user community.

Modeling Approach

In order to compute the coupling effects occurring in a magnetic bearing, two loops have been implemented, see Fig. 1. The first loop simulates the interaction between rotor motion and electromagnetic field including the controller. Furthermore, the heating of the rotor d.t.

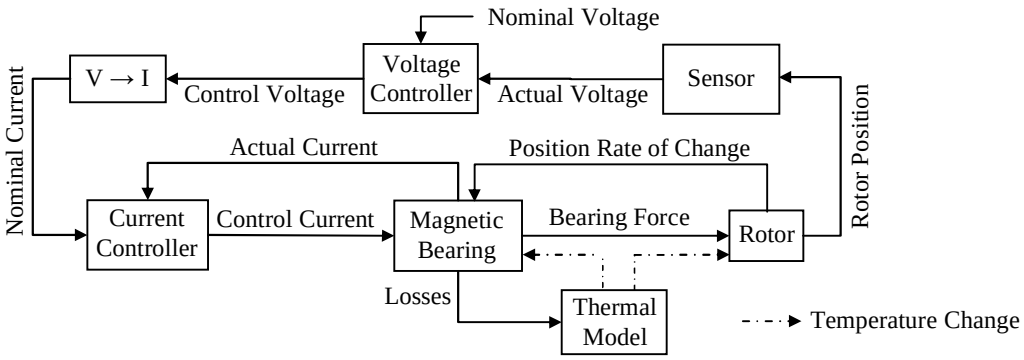

Fig. 1: Sketch of the multiphysical coupling of magnetically levitated rotors

electromagnetic losses is used to determine the change of mechanical, thermal and electromagnetic properties and the resulting effect on bearing forces, losses and rotor behavior are considered.

Electromagnetism. In order to determine the bearing forces and losses, FEMM (finite elements method magnetics) is used, which solves Maxwell's equations for linear and non-linear magnetic materials. The force computation is already implemented in FEMM by solving Maxwell's stress tensor. The losses are computed applying harmonic analyses [4,5]:

$$P = \sum_{k=0}^{\infty} \left\{ -\pi \Omega d k^2 \, \mathrm{Im}(\mu_k) \coth\left[\frac{k}{r_o}(r_o - r_i) \right] \frac{|a_k|^2}{|\mu_k|^2} \right\}, \tag{1}$$

where Ω is the rotor speed, d is the lamination thickness in the rotor, r_o and r_i are the outer and inner radius of the rotor, respectively. In order to take hysteresis effects into account, a complex permeability approach is used to determine the magnetic permeability representing the k^{th} harmonic μ_k [6]. Since FEMM is not feasible for harmonic analyses, the algorithm has been coupled to Matlab to compute the k^{th} harmonic of the vector magnetic potential a_k.

The parametric model is currently limited to heteropolar bearings and is feasible for arbitrary number of poles, geometry and windings. Examples of different stator geometries and the resulting losses are plotted in Fig. 2. It becomes obvious that the total losses can be reduced when reducing the number of magnetic poles, i.e. NNSS configuration, or the number of stator poles (e.g. six poles). The latter yields drawbacks regarding control algorithm complexity.

Rotordynamics. In order to model the flexible shaft of a magnetically levitated rotor, the Jeffcott rotor approach is applied, see Fig. 3 a). In the developed algorithm, the number of shaft elements n_S and discs n_D can be chosen arbitrarily. Generally, the resulting differential equation can be written as

$$\mathbf{M}\underline{\ddot{x}} + (\mathbf{G}\Omega + \mathbf{D})\underline{\dot{x}} + (\mathbf{G}\dot{\Omega} + \mathbf{C})\underline{x} = \underline{F}_{\mathrm{MB}} + \underline{F}_{\mathrm{Dis}}, \tag{2}$$

where **M**, **G**, **D**, and **C** denote the inertia, gyroscopic stiffness, damping and flexibility of the rotating shaft, respectively. The rotor motion is represented by the vector $\underline{x}$ and the external forces/torques d.t. bearings and disturbances are represented by $\underline{F}_{\mathrm{MB}}$ and $\underline{F}_{\mathrm{Dis}}$. The Jeffcott rotor model is mostly applied to virtually infinite stiff bearings. In order to include finite

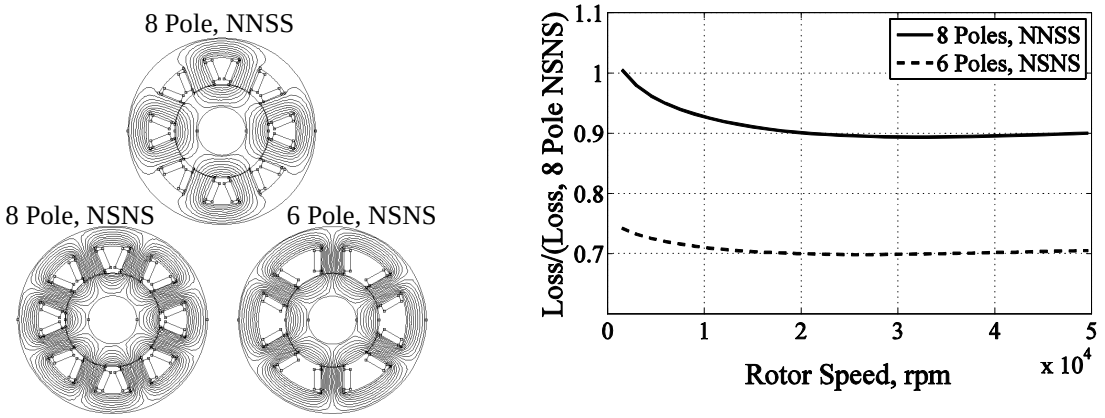

a) Bearing configurations b) Comparison of bearing losses

Fig. 2:Different magnetic bearing configurations and loss analysis

bearing stiffness, the stiffness matrix has to be extended to

$$\mathbf{C} = \begin{bmatrix} \mathbf{C}_\mathrm{R} & \mathbf{C}_\mathrm{R}\mathbf{T} \\ \mathbf{T}_\mathrm{MB}\mathbf{C}_\mathrm{R} & \mathbf{T}_\mathrm{MB}\mathbf{C}_\mathrm{R}\mathbf{T} \end{bmatrix}, \tag{3}$$

where $\mathbf{C}_\mathrm{R} \in \mathrm{IR}^{4(n_\mathrm{S}+n_\mathrm{D})\times 4(n_\mathrm{S}+n_\mathrm{D})}$, $\mathbf{T} \in \mathrm{IR}^{2n_\mathrm{MB}\times 4(n_\mathrm{S}+n_\mathrm{D})}$ and $\mathbf{T}_\mathrm{MB} \in \mathrm{IR}^{4(n_\mathrm{S}+n_\mathrm{D})\times 2n_\mathrm{MB}}$. $\mathbf{C}_\mathrm{R}$ includes the shaft flexibility that is determined via Euler–Bernoulli or Timoshenko beam theory, see e.g. [8]. The transformation matrices $\mathbf{T}$ and $\mathbf{T}_\mathrm{MB}$ represent the geometric coupling between the shaft elements and the bearings. In order to provide arbitrary geometries of the rotor, the bending line is solved symbolically. Since flexible hubs can enhance the system performance by allowing for tilted rotation of discs, the algorithm is also feasible for hubs represented by a linear torsional spring.

Thermodynamics. For the thermal modeling, heat conduction, heat transfer, radiation, and external heat sources (losses) are taken into account (since vacuum applications are studied, convection is neglected). In order to calculate the rotor temperatures, the energy balance of a axisymmetric volume element consisting of an incompressible medium is considered:

$$\dot{T}\left(c_p T \frac{\partial \rho}{\partial T} + \rho T \frac{\partial c_p}{\partial T} + \rho c_P \right) = \frac{\partial \lambda}{\partial T}\left[\left(\frac{\partial T}{\partial r} \right)^2 + \left(\frac{\partial T}{\partial z} \right)^2 \right] + \lambda \left(\frac{\partial^2 T}{\partial r^2} + \frac{\partial^2 T}{\partial z^2} \right) + \frac{\lambda}{r}\frac{\partial T}{\partial r}. \tag{4}$$

This volume element is described by its mass density ρ, the thermal capacity c_p, the thermal conductivity λ and the temperature T. The radiation heat flux $\dot{q}_\mathrm{R}$ and external heat sources $\dot{q}_\mathrm{ex}$ occurring at the walls (index W) are included via the Neumann boundary condition, $\dot{q}_\mathrm{R/ex} = \frac{\partial T}{\partial x}\big|_\mathrm{W}$. Herein, x denotes the surface normal, i.e. r and z depending on the surface orientation. The heat transfer between two components is described via Robin boundary condition for the elements on both sides of the wall (indices + and –), $\alpha\left(t_{\mathrm{W}+} - t_{\mathrm{W}-}\right) = \frac{\partial T}{\partial x}\big|_{\mathrm{W}-}$ and $\alpha\left(t_{\mathrm{W}-} - t_{\mathrm{W}+}\right) = \frac{\partial T}{\partial x}\big|_{\mathrm{W}+}$, respectively. Eq. (4) is solved via finite difference method and an alternating direction implicit procedure [9]. In Fig. 3 b), an example result plot of the thermal analysis is shown. The indicated components and regions are only representative examples.

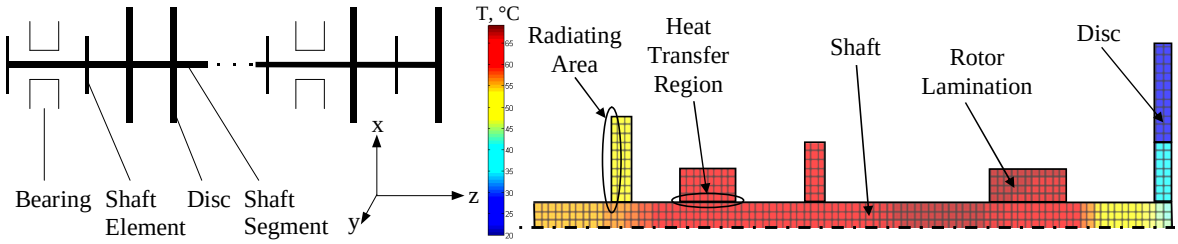

a) Jeffcott rotor model b) Thermal model

Fig. 3: Mechanical and thermal model. a) Schematic of the Jeffcott rotor model. The shaft inertia is represented by shaft elements whereas the flexibility of the shaft is included in the shaft elements. Additionally, superstructures can be included as discs. b) Example result plot of the thermal model indicating different thermal regions.

Controller. As indicated by Fig. 1, the implemented controller model (analog signal processing) consists of sensors (represented by PT1 elements), voltage controllers, V-to-I converters (represented by PT1 elements), and current controllers compensating transient effects in the bearing coils. Current control has been chosen, since it is less complex and more established when compared to voltage control [10].

Integration of the Overall Model. The coupling between electromagnetism (FEMM) and rotordynamics/thermodynamics/controller (Matlab) is performed via the open source software Octave. First attempts for direct coupling during computation yielded unacceptable computation times. Hence, look-up tables (LUT's) are implemented in the algorithm. The data flow of the algorithm is depicted in Fig. 5. In order to provide adequate results and computation times, the step size for the LUT's has to be chosen carefully.

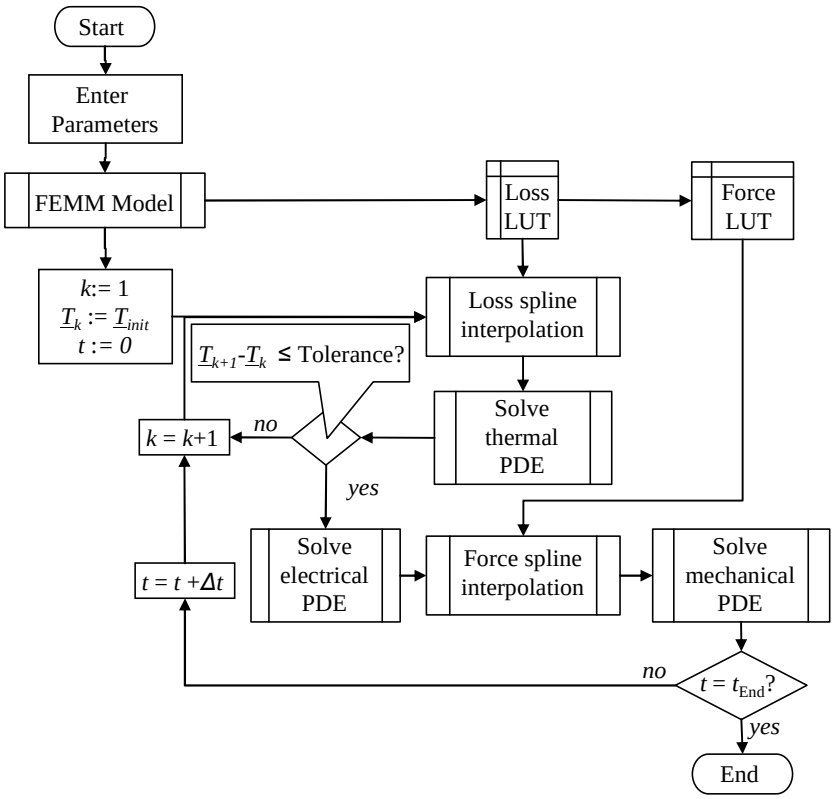

Fig. 4: Flow chart of the implemented multiphysical coupling [11]

MagBeS

MagBeS bases on a graphical user interface, where the geometric, electromagnetic and material properties can be entered and the required analyses can be selected. Different analyses (transient, steady-state, frequency domain) and a variety of result plots can be generated (e.g. Campbell diagram, Bode plot, temperature field, transient characteristics of currents…). For the design of a magnetically levitated rotor, various boundary conditions that are especially of importance for space applications (e.g. volume, power consumption, mass) can be entered. It should be noted that the design feature of MagBeS is supposed to be sufficiently accurate for rough dimensioning of the system but does not yield a final design. It is especially useful to compare different design options.

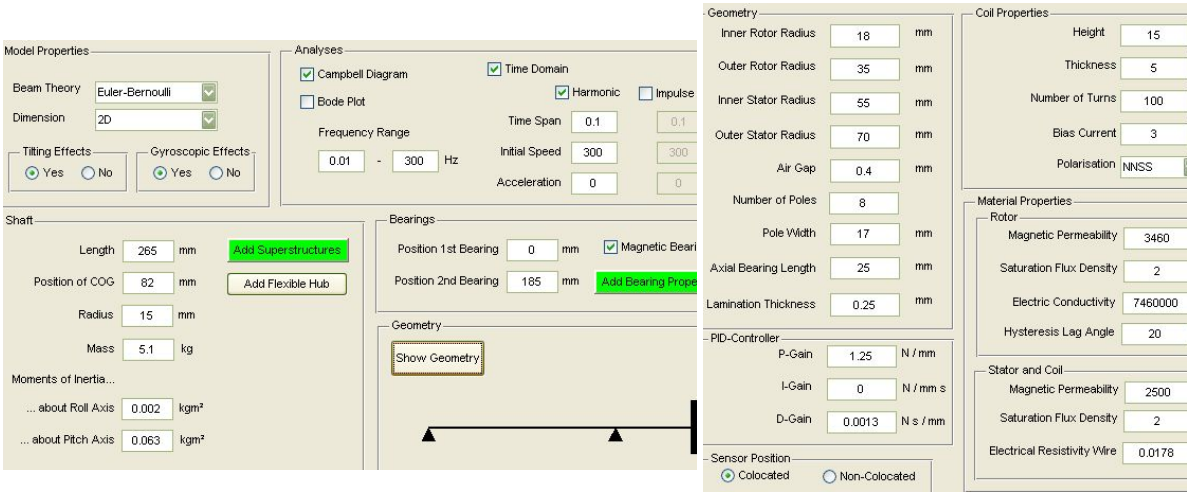

Fig. 5: Examples of the Graphical User Interface of MagBeS

Model Evaluation

A test rig consisting of two radial and one axial magnetic bearing is used to validate the numerical models, see figure 6. It monitors the shaft temperature at different positions, braking torques, power consumption and the rotor motion. The rotor is run in vacuum to eliminate air friction.

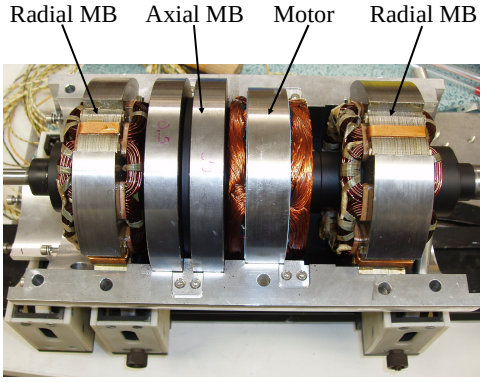

Fig. 6: Interior view of the test rig

Table 1: Properties of the Test Rig

mechanical properties	shaft length	≈ 380 mm
	bearings	2 radial, 1 axial MB
		2 touchdown bearings
	rotating mass	≈ 12 kg
	rotor radius	≈ 15 mm
	disc radius	≈ 350 mm
	speed range	0-21,000 rpm
MB properties	bearing types	radial: heteropolar
		axial: homoploar
	air gap	400 µm
	bias current	variable (reference 3 A)

During acceleration of the shaft, the eigenfrequencies have been determined to be approx. 65 Hz and 105 Hz, respectively. The computed eigenfrequencies are at 60 Hz and 110 Hz. Hence, the deviation is less than 10 %. The losses have been measured during rundown tests. They are approx. 5 W at 100 Hz and 25 W at 300 Hz. The occurring computation errors are less than 20 %. Furthermore, the thermal behavior has been measured during operation. Comparison with computation results showed deviations below 10 %.

Simulation Results

A variety of sensitivity analyses has been performed, in order to find design criteria and to evaluate different solutions. As examples, the results of two analyses that take advantage of the presented coupled algorithm are plotted in Fig. 7. The considered reference system consists of two radial magnetic bearings and an overhanging disc, see Fig. 7 a). One of the bearings is situated closed to the centre of gravity of the whole rotor system. As already mentioned, the integration of a flexible hub can improve the performance of the system. In Fig. 7 b), the required control current of one bearing is plotted as a function of time for a harmonic excitation d.t. shaft imbalance. It becomes obvious that the required control current can be almost halved when allowing for some disc tilting.

The second analysis shows the impact of the bias current on the electromagnetic losses occurring in the magnetic bearing and the resulting maximum shaft temperature. It can be seen that large bias currents can yield temperatures that are critical for some rotor elements, such as motor magnets. For this analysis, only the bias current of the right bearing has been changed, i.e. when also reducing the current in the left bearing, the temperatures can be reduced even more.

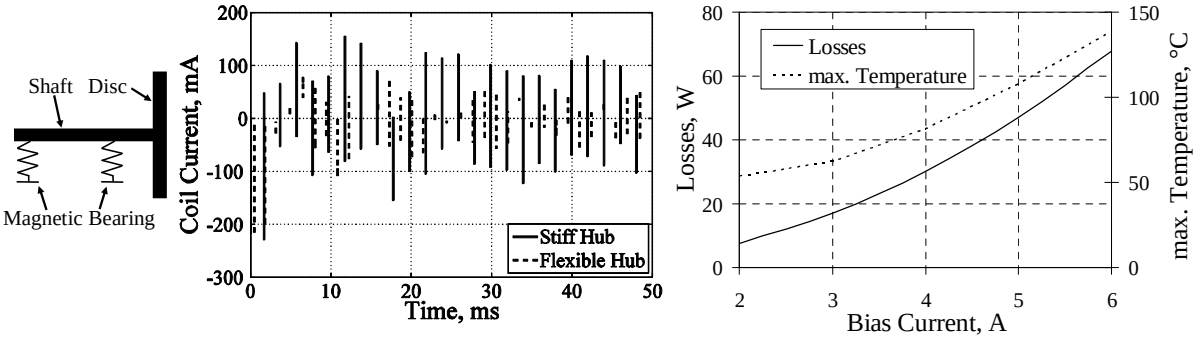

a) Reference System b) Coil Current of shaft with flexible hub c) Loss and temperature vs. bias current

Fig. 7: Examples of coupled analysis at 300 Hz. a) Pictogram of the reference system b) Required coil current for a system with and without a flexible hub. c) Loss and temperature as a function of the bias current

Conclusions and Outlook

The developed parametric algorithm is feasible to investigate electromagnetism, rotordynamics, thermodynamics as well as controller properties of active magnetically levitated rotors. Comparison to measurements has shown that the algorithm results yield good conformance.

The implementation of a graphical user interface, called MagBeS (Magnetic Bearing Simulator), has been carried out, in order to provide a user-friendly handling. The tool can be

used to analyze and design magnetic bearings. In order to improve the implemented design approach, the applicability of genetic algorithms is currently under investigation.

Acknowledgment

This study is supported by Astrium GmbH Friedrichshafen in the frame of the Research Training Group (Graduiertenkolleg) “Aspects of Future Satellite Reconnaissance Missions”.

References

[1] P. A. Studer, IEEE Transactions on Magnetics, vol. 13, no. 5, pp. 1155-1157, September 1977.
[2] C. H. Henrikson, J. Lyman, and P. A. Studer, AIAA Paper,AIAA Paper, no. 1974-128, 1974.
[3] A. Pilat, “Automatic Generation of Active Magnetic Bearing Geometry with COMSOL Multiphysics”, Proc. of the COMSOL Users Conference 2007, Grenoble, 2007.
[4] R. L. Stoll, The analysis of eddy currents. Oxford: Clarendon Press, 1974.
[5] D. Meeker and E. Maslen, Journal of Tribology, Vol. 120, No. 3, 1998, pp. 629-635.
[6] D. Meeker, A. V. Filatov, and E. Maslen, IEEE Transactions on Magnetics, Vol. 40, No. 5, pp. 3302-3307, 2004.
[7] D. Meeker, Finite Element Method Magnetics Version 4.2. User’s Manual, pp. 7-8, 2007.
[8] F. F. Ehrich, Handbook of Rotordynamics, New York: McGraw-Hill, 1992.
[9] J. Douglas and H. H. Rachford, Transactions on the American Mathematical Society, Vol. 82, No. 2, pp. 421-439, 1956.
[10] G. Schweitzer and E. Maslen, Magnetic Bearings – Theory, Design and Application to Rotating Machinery, Berlin: Springer, 2009, pp. 48-51.
[11] A. Deckert, U. Keller, and S. Fasoulas, “A Parametric Approach for Multiphysical Modeling of Magnetic Bearings”, IEEE Transactions on Magnetics, submitted for publication, 2010.